



Productivity of Solar Still Unit Engaged with Waste Energy Source

Omar A. Elfiiky, Ramdan Y. Sakr, Ghazy M. Assassa, Mohamed R. Salem

Mechanical Engineering Department, Faculty of Engineering at Shoubra, Benha University, 108 Shoubra St., Cairo, Egypt

Abstract: This work aims to improve the productivity of solar still unit (SSU) by multiplying the supplied heat energy. Experiments are carried out daily from 10 AM to 3 PM using heating air, which simulates the exhausted gases from engines, boilers, or any other source. Several mass fluxes (up to 63.5 kg/s.m^2) of the air beneath the solar still unit are tested at constant inlet temperature. The results state that just applying the proposed external heating system augments the accumulated yield while the thermal efficiency is decayed when compared with the unmodified unit. Besides, increasing the heating air flow rate boosts both the system productivity and thermal efficiency. Another part of the experiments is occurred for the whole day with heating air system at mass flux of 63.25 kg/s.m^2 . For the modified unit, the outputs state that the change in the temperatures and freshwater yield are small along the day when compared with the reference one, in which the temperatures reach their peak values at 1 to 1:30 PM. The resulted accumulated yield over the whole day is increased from 3.16 l/m^2 for the reference unit to be 13.48 l/m^2 . This increase corresponds to an enhancement ratio of 326.6%.

Keywords: Solar still; Waste energy; Performance; Distillation.

1. Introduction

Nowadays, numerous countries face a significant shortage in saving freshwater sources that required for drinking or for industrial processes needed for the development [1]. Although all quantity of water on the earth's surface is about 326 million trillion gallons, the oceans consist of 96.5% from this amount, while less than 3% of this quantity represents the freshwater (suitable water for drinking). This statistic shows how the quantity of freshwater is so small. So, all the world tends to present new desalination approaches to provide suitable water for agriculture, industry, and drinking. There are at least three basic methods of desalination; thermal, pressure and electrical. The solar module is an artificial water purifier to purify brackish water; The sun drives the distillation process. The units make use of solar energy instead of fossil fuels to produce pure water vapor. The pure water vapor is then collected and condensed into a liquid form as it cools [1, 2].

In the direction of configuration improvement, Abu-Arabi et al. [3] replaced the single-glass cover with a double one to increase the temperature difference between the water in the basin and glass surface, which augmented the rate of freshwater production. Radhwan[4]used built-in phase change material (PCM) through stepped SSU, while Mettawee and Assassa [5]studied the impact of feedwater flow rate and layer thickness of PCM on heat amount absorbed. Abdel-Rehim and Lashine

[6] utilized the rejected heat energy from a condenser of an air conditioning system as an additional heat source for still beside the sun. Improving the performance of SSU by placing a wet wick on one of the glass plates to lower its temperature was executed by Sandeep et al.[7]. The productivity was expanded by 46.7%. El-Sebaï and El-Naggar [8]improved the SSU performance by using finned-basin and changing the material of the fins; copper, glass, aluminum, iron, mica. Hansen and Murugavel[9] employed a hot water storage tank and inclined SSU with three variable absorber forms; flat, grooved, and fin shaped. Deshmukh and Thombre [10] experimentally investigated single slope SSU combined with passive thermal storage medium (oil and sand) where the solar energy, all day, was transferred by the oil to the sand, which acts as a heat source for saltwater at night. Faegh and Shafii[11] employed an evacuated-type solar collector to heat the feedwater, besides using PCM, while Harahsheh et al. [12]researched the performance of an SSU equipped with a flat solar collector in a closed-loop hot water circuit with employing PCM. Sharshir et al. [13]worked on enhancing the SSU performance by employing a nanofluid, but Rufuss et al. [14] utilized nanoparticles with PCM, which showed an enhancement in the still productivity over using PCM only. An SSU equipped with heat exchangers and nanofluid as a working medium was

introduced by Mahian et al.[15]. They discussed the effect of varying

the size of particles, level of the saline water in the basin, and nanofluid flow rate on the performance. Compared with traditional SSU, Shadi et al. [16] achieved an increase in productivity and efficiency due to using a sloping staged still configuration of 28 trays. Poblete et al. [17] combined a solar air heater and solar collector with an SSU, while Kabeel et al. [18] investigated inclined SSU with traditional solar. Kabeel and Abdelgaied[19] worked on reinforcing the performance of a pyramid SSU by using an absorber surface made from graphite to enable the absorber to store more heat during high solar energy time and get it back to the basin's water during sunset. Manokar et al. [20] used a new technique to get distilled water from saline water by cooling the photovoltage cell, where they used a solar cell as a basin for inclined SSU. Shehata et al. [21] attached ultrasonic humidifiers, PCM, and reflector besides an evacuated solar collector to an SSU. Salem et al. [1] tested different densities and thicknesses of a floating sponge on the SSU performance. The cost was reduced by 35% at optimum case. On the other side, the impact of the feedwater level inside the solar basin on productivity was shown by El-Maghlany et al. [22]. Generally, there are several approaches suggested to augment heat transfer rates [23-26]. This work suggests a new enhancement approach for the solar still yield. It is a well-known that there is a huge amount of thermal waste energy delivered to the atmosphere from numerous industrial applications. This waste energy has bad

effects on the ambient, in addition to losing the money that was spent

on heating the source of that energy. Therefore, this work simulates the waste energy and uses it as another source for heating the saline water in the basin. Several flow rates of the heating air flowing in a duct behind the still are tested. The results are exposed in terms of the SSU operational conditions besides its yield and efficiency.

2. Experimental setup and procedures

In the present study, two stills are compared together simultaneously. One of them is a conventional, while the other is equipped with a heating air duct (Fig. 1). The conventional still consists of a 2mm thickness black steel basin, having base area of 1x1 m², and four sides of 20cm height. A wooden box of thickness 10 mm surrounds the basin sides with a gap 10 mm to thermally insulate it. The gap between the basin and the wooden box is filled with polyurethane foam to act as additional insulation. The upper face of the basin is black, while all sides are white painted to strengthen reflectivity to reduce heat loss. There are two holes in the basin; one of them to get out the slats and washing water to the brine tank, while the other gets out fresh water. The basin is left to a height of 60 cm through wooden legs and covered with a glass cover consists of four glass plates, two of them are identical plates with 4 mm thickness (transmissivity of 91%), and dimensions of 970 mm x 565 mm. These plates are inclined by an angle 30° with the horizontal. The other two plates are vertical plates of a triangle shape.

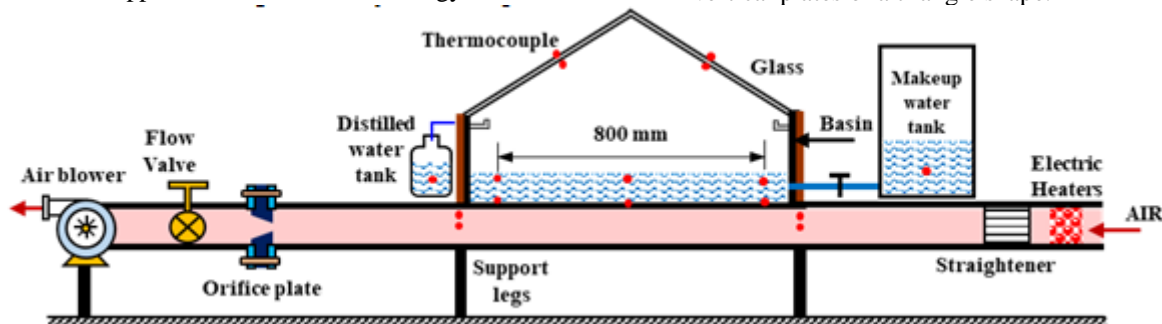


Fig. 1: A schematic diagram of the tested SSU engaged with the air duct.

The inclined glass cover behaves as a condensation surface for the evaporated water, besides a closed barrier between the water vapor inside the basin and the outside. The condensed vapor is gathered through tray, which consists of 4-semi-circular PVC pipes (1.5-inch in diameter and 1 m in length) bolted at the basin's vertical sides. The tray inclines by a total distance of 8cm to guide the condensate water to the outlet port. A glass vessel is used to store and calibrate the distillate water, where it graduates in millilitres. The vessel is connected to the outport by PVC pipe tighten well to prevent any leakage. Moreover, this vessel is coated by a layer of glass wool having a

thickness of 1 inch. The source of the saline water is a cylindrical tank, 2 mm steel thickness, with a capacity of 20 litres. The other still has the same configuration as the conventional, but it is supported on a 2 mm wall thickness galvanized steel duct through which the heating air passes. The tunnel is formed as a rectangular shape with dimensions of 1000x80*3000 mm. The outer surface of the tunnel is thermally isolated to diminish the heat loss to the atmosphere. To simulate the hot industrial fumes, seven circular electric- heaters (6.3 kW total capacity) are fitted at the entrance of the duct in staggered order to heat the entering air to a temperature of 135°C adjusted

by a thermostat. This value of temperature corresponds to the flue gases' temperatures of many thermal applications such as:

- For coal-fired power plant units, the flue gas temperature of boilers can reach 120-150°C[27].
- Flue gas from household gas water heater has a range of 110-160°C [28].
- Flue gas from gas boiler ranges between 90°C and 130°C[28].
- Flue gas from natural gas power plant ranges between 90°C and 150°C[28].
- Flue gas from thermal power station ranges between 90°C and 140°C[28].

Additionally, a straightener is employed next to the heater to provide uniform flow. The area of the top surface of the duct over which the still is supported (at distance 1200 mm from entrance) is cut to provide direct contact between the hot air the base as shown in Fig. 2. After leaving the main duct, the air enters the metering duct via the transition section, which is formed as a converging section. The metering duct comprises two PVC pipes and orifice plate which were designed according to Miller [29]. A three-horsepower blower is used to move the hot air inside the duct. A sliding gate is installed to control the airflow through the duct.

Twenty-eight K-type thermocouples (wires of 0.2 mm diameter) are incorporated in the two units to

measure the temperatures at various locations as indicated in Fig. 1. The output terminals of thermocouples are connected to digital temperature indicator with resolution of 0.1°C through a junction box. Hot airflow rate is estimated by measuring the pressure drop across the calibrated flow-orifice meter by a digital manometer of accuracy of ± 1 Pa. The incident solar radiation intensity is measured in watts per meter squared of the SSU base (W/m^2) by a digital solar power meter, which has a range of 0-2000 W/m^2 and accuracy of $\pm 5\%$ of reading or ± 10 W/m^2 . The surrounded conditions (humidity, wind speed, and ambient temperature) are measured by a digital-environmental meter. The salinity of the salt feed water and the distillate water is measured by a multiparameter meter (code: HI9829) with accuracy of ± 10 ppm.



Fig. 2: Duct configuration.

3.Experimental procedures

All rig investigations are carried out at Faculty of Engineering at Shoubra, Cairo, Egypt

(30.1° N Latitude) through June 2021. The experiments begin in period (10:00 AM to 3:00 PM) each day, except for two days, in which the runs start from 8:00 AM until next 8:00 AM. At the start of each trial, some steps are carried in order as follows:

- 1) Washing and cleaning the two glass plates and the basin well from any contaminations due to the last investigation.
- 2) Refilling saline-water reservoir to the setpoint level.
- 3) Checking all the thermocouples at their locations.
- 4) Before turning on the power, all the electric heaters and blower's motor are checked well then, the hot-air thermostat is set at 135°C. The system operates daily at 8:30 AM, and the first reading is taken at 10 AM.

The following parameters: wind speed, incident solar radiation, temperatures of the system (base, saline water, inlet/outlet air, and glass), and dry-bulb temperature of ambient are recorded at each reading, every 30 minutes. Also, the feed water thermostat is set according to the value of the basin water every 15 minutes.

4.Calculations

Series of relations are utilized to detect and calculate the performance of both units, where T_b , T_{sw} , $T_{a,i}$, $T_{a,o}$, and T_g are calculated through relations which employ the observed values and their readings number as follows:

$$T_b = \frac{\sum T_{b,i}}{3} \quad (1)$$

$$T_{sw} = \frac{\sum T_{sw,i}}{3} \quad (2)$$

$$T_{a,i} = \frac{\sum T_{air,i}}{2} \quad (3)$$

$$T_{a,o} = \frac{\sum T_{air,o}}{2} \quad (4)$$

$$T_g = \frac{\sum T_{g,i}}{4} \quad (5)$$

Where the locations of the thermocouples represented by index i . Eq. (6) calculates the daily accumulated water by summing the instantaneous distilled water during the operating time (OT), while Eq. (7) presents the percentage of enhancement for distilled water produced from the system.

$$V_{dis,d} = \sum_1^{OT} V_{dis,i} \quad (6)$$

$$\Delta V_{dis} (\%) = \left[\frac{V_{dis,d,mod} - V_{dis,d,ref}}{V_{dis,d,ref}} \right] \times 100 \quad (7)$$

The thermal immediate efficiency of the SSU ($\eta_{th,i}$) is presented as the energy required for producing the distillate water over the total input energy; Eq. (8), where ($h_{fg,i}$) is estimated at the temperature of the saline water, T_{sw} , using Eq. (9), which is acceptable for temperature range (0°C-200°C) [30].

$$\eta_{th,I} = \frac{\left[\frac{\rho_{dis,I} V_{dis,I} h_{fg,I}}{t_G} \right]}{S_I A_b + \dot{m}_a C p_a (T_{a,i} - T_{a,o})} = \frac{\rho_{dis,I} V_{dis,I} h_{fg,I}}{[S_I A_b + \dot{m}_a C p_a (T_{a,i} - T_{a,o})] (0.5 * 3600)} \quad (8)$$

$$h_{fg,sw} = 1000 [2501.9 - 2.40706 T_{sw} + (1.192217 * 10^{-3} T_{sw}^2) - (1.5863 * 10^{-5} T_{sw}^3)] \quad (9)$$

Also, the thermal efficiency per day for the SSU ($\eta_{th,d}$) is obtained as follow:

$$\eta_{th,d} = \frac{\sum_1^{OT} \left[\frac{\rho_{dis,I} V_{dis,I} h_{fg,I}}{t_c} \right]}{\sum_1^{OT} [S_I A_b + \dot{m}_a C p_a (T_{a,i} - T_{a,o})]} \quad (10)$$

The air mass flux (ϕ) through the tunnel beneath the distillation unit is calculated as follows;

$$\phi = \frac{\dot{m}_a}{A_{duct}} = \frac{\dot{m}_a}{w * H} \quad (11)$$

The uncertainties in the produced freshwater and in its change are reported as ± 10 ml and 0.6%, respectively. Besides, the uncertainties in the instantaneous and daily thermal efficiency are reported as 6.2% and 2.3%, respectively.

5. Verification of the SSDUs output similarity

Because the reference and modified SSUs are tested in parallel, their yields are compared under the same operating conditions for non-engaging the external heating source to verify their similarity. It is seen in Fig. 3 that there are tiny deviations between the yield of both units (maximum deviation of $\pm 1.7\%$), which say that they are identical and can be compared at dissimilar working conditions.

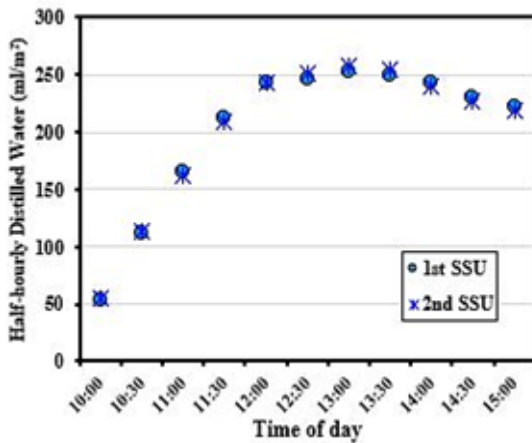


Fig. 3: The yield of the two SSUs under the same conditions.

6. Results and discussions

6.1 Operational principle of the SSUs

In this section, the operational principle of the SSU with/without using the heating air is illustrated. Fig. 4 reports the instantaneous temperatures for the two tested SSUs; reference and modified unit for mass flux of 37.63 kg/s.m² as a sample of the outputs.

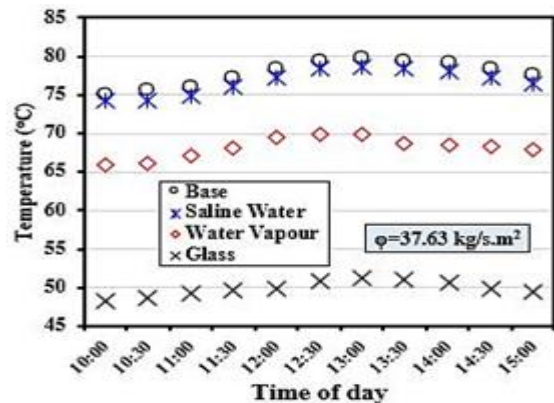
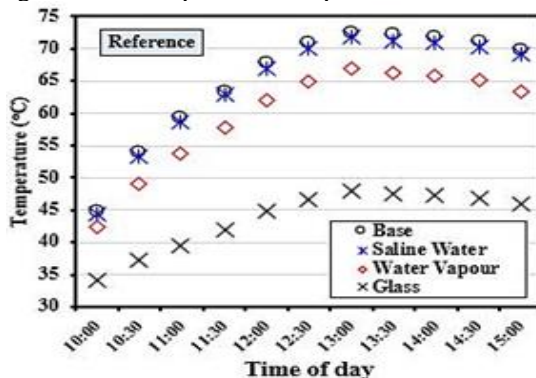


Fig. 4 The instantaneous temperatures in the distillation units.

In both units, the basin base owns the peak temperature; the base plate absorbs the solar radiation from top surface, besides the heat energy coming from the heating air beneath the basin, and then heats up the brackish water in the basin by free convection and thermal radiation emitted to the solid particles in the water. This drives this water to evaporates; the produced vapor is then condensed on the inside surface of the glass covers which have lower temperatures. A clear note in the results is that the change in system temperatures during the day is negligible in the case of the treated unit, and the temperature changes in the reference unit increase during the day, as these changes correlate with the change in intensity of solar radiation.

6.2 Effect of engaging external heating source

In this part, the behaviour of the system temperatures is presented due to conducting the heating air tunnel beneath the SSU. Fig. 5 shows the average effect of the airflow mass flux on the system temperatures. These results are the average values for the runs carried out between 10 AM to 3 PM. The results indicate that as soon as hot air passes under the unit, temperatures in the system increase. Besides, the increases in the system temperatures are raised by increasing the air mass flux. It is seen that the base temperature is increased from 65.3°C in the reference SSU to be 73.8°C and

81.8°C at mass fluxes of 15 and 63.25 kg/s.m², respectively. The corresponding water vapor temperatures are 59.8°C, 66.5°C and 70.2°C, respectively. It is seen also that there is a significant increase in the glass temperature by increasing the heating air mass flux. The average temperature of the glass is increased from 43.6°C in the unmodified SSU to be 48.6°C and 51.6°C at mass fluxes of 15 and 63.25 kg/s.m², respectively. This behaviour is due to increasing the heat transfer rate by increasing the air flow rate. Thus, the base temperature is raised which augmented the heat exchange between the base and the saline water, and consequently the water vapor and glass temperatures are raised.

Moreover, Fig. 6 introduces the average yield and thermal efficiency over the same period; from 10 AM to 3 PM. The freshwater productivity is significantly augmented because of conducting the waste heat energy system, and this enhancement is boosted by increasing the air flow rate. The resulted average accumulated yield is 2.23 l/m² produced by the unmodified unit, while the yield is increased to be 2.53 and 3.98 l/m² with using heating air at mass fluxes of 15 and 63.25 kg/s.m², respectively. Compared with the reference unit, the corresponding enhancements in the yield are 13.2% and 78.3%, respectively

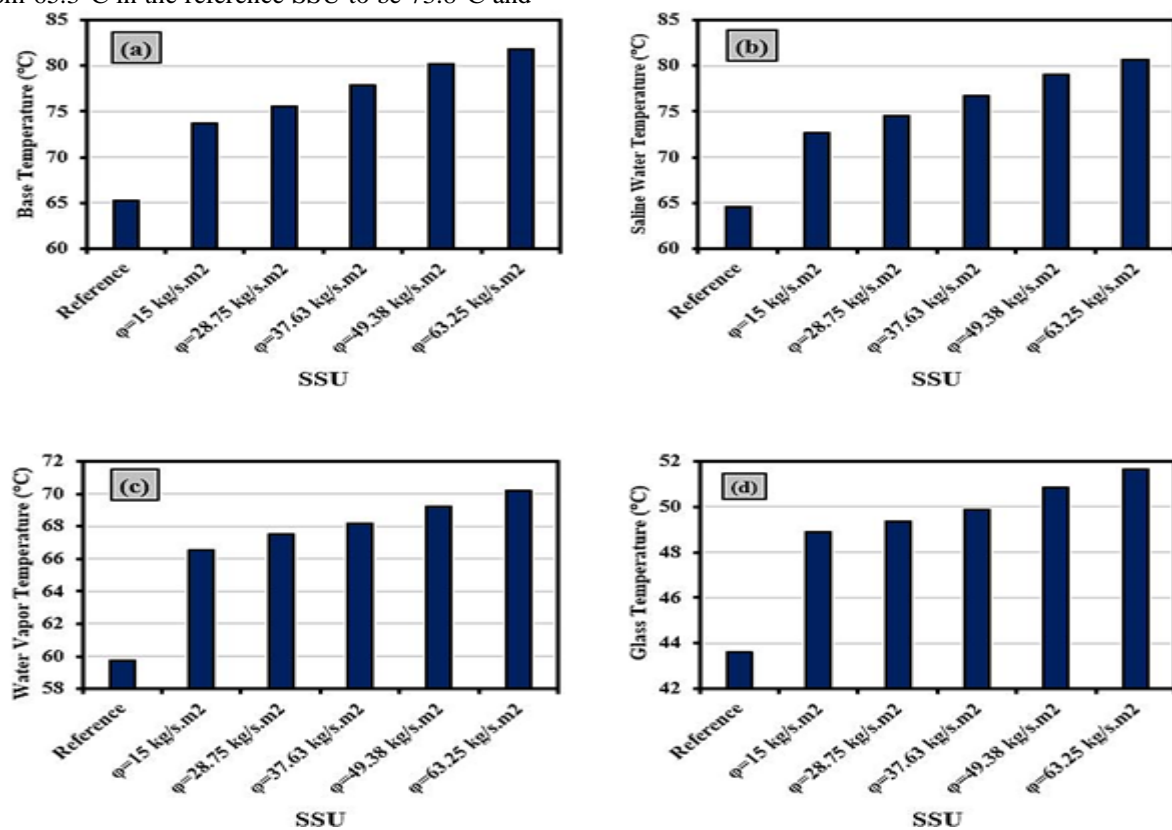


Fig. 5 Average temperatures at different heating airflow rates (10 AM to 3 PM).

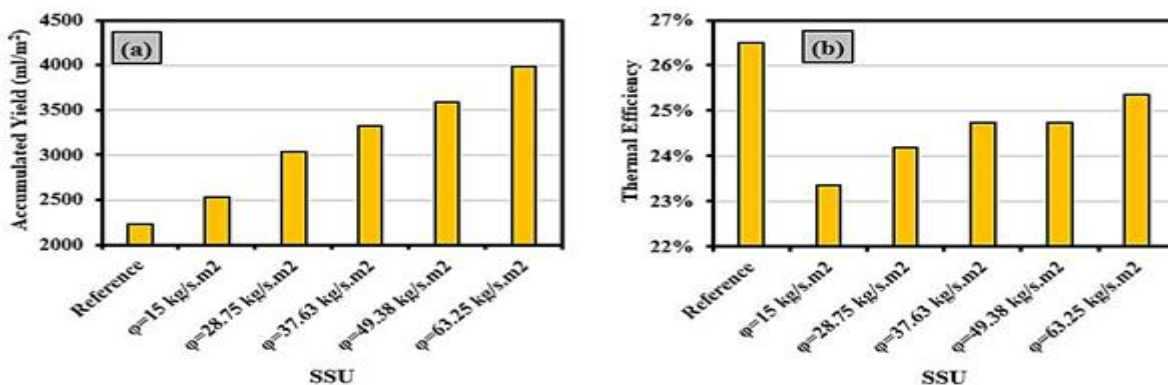


Fig. 6 Average performance attributes at different heating airflow rates (10 AM to 3 PM).

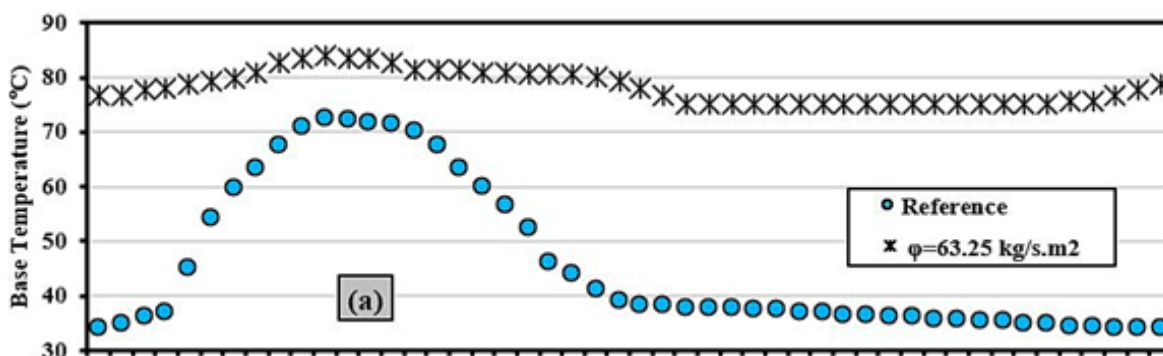
Additionally, although the yield is improved by engaging the external heating source, the thermal efficiency of the unmodified unit is higher than the others. The results show that the average thermal efficiency of the reference SSU is 26.5%, while by conducting heating air beneath the unit, the average thermal efficiency becomes 23.4% and 25.4% at mass fluxes of 15 and 63.25 kg/s.m², respectively. This means that not all the water vapor formed (with engaging an external heating source) has condensed, and this may be due to an increase in the temperature of the glass. Moreover, although the increase in the air flow led to a further increase in the temperature of the glass, the thermal efficiency improved slightly, and this may be due to the significant increase in the production of water vapor.

6.3 Performance of the SSU over the whole day

In this section, the performance attributes are presented for the unmodified unit beside the SSU engaged with external heating source with airflow at 63.25 kg/s.m². Fig. 7 demonstrates the system temperatures while Fig. 8 presents the freshwater productivity and thermal efficiencies of both units for a complete day, which starts at 8 AM and finishes the same time in the next day. For the modified unit, the outputs state that the change in the temperatures is small along the day when compared with the reference one, in which the temperatures reach their peak values at 1 to 1:30 PM. This is reflected in unit productivity, as the yield of modified unit

changes little during the day, dropping more often between 7 and 11 PM. Then it settles in at night until 6 AM. On contrary for the reference unit, in which the yield significantly changes during the day, where it follows the intensity of solar radiation. Its productivity peaks at 1PM, and productivity decreases over time before/after this time; it should be noted that there is no yield between 6 PM to 9 AM. The resulted accumulated yield over the whole day is increased from 3.16 l/m² for the reference unit to be 13.48 l/m² for the unit engaged with heating air system at mass flux of 63.25 kg/s.m². This increase corresponds to an enhancement ratio of 326.6%.

Considering the thermal efficiency, it directly follows the intensity of solar radiation in the case of the reference unit; it is small at the beginning of the day and gradually increases with the increase in solar radiation and reaches its maximum value at the noon and gradually decreases until the sun sets, after which it is equal to zero until the beginning of the next day. For the modified unit, the thermal efficiency is nearly stable over the day, except a short period (7 to 8 PM), which owns a relatively higher efficiency. This may be due to decreasing the temperature of the glass which augments the condensation process. Furthermore, at this period, there is accumulated heat energy stored in the saline water in the basin, which enhances the thermal efficiency of the system at this period.



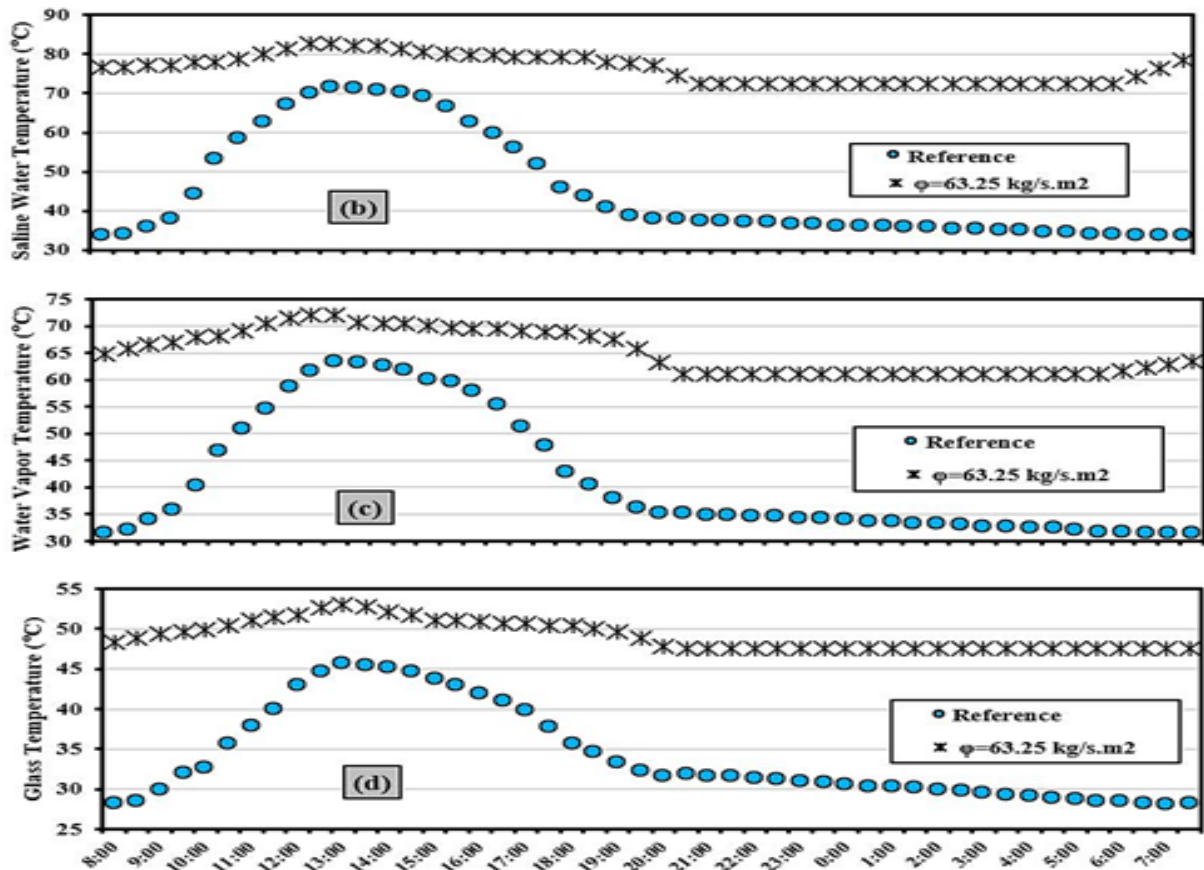


Fig. 7 System temperatures during 24-hours.

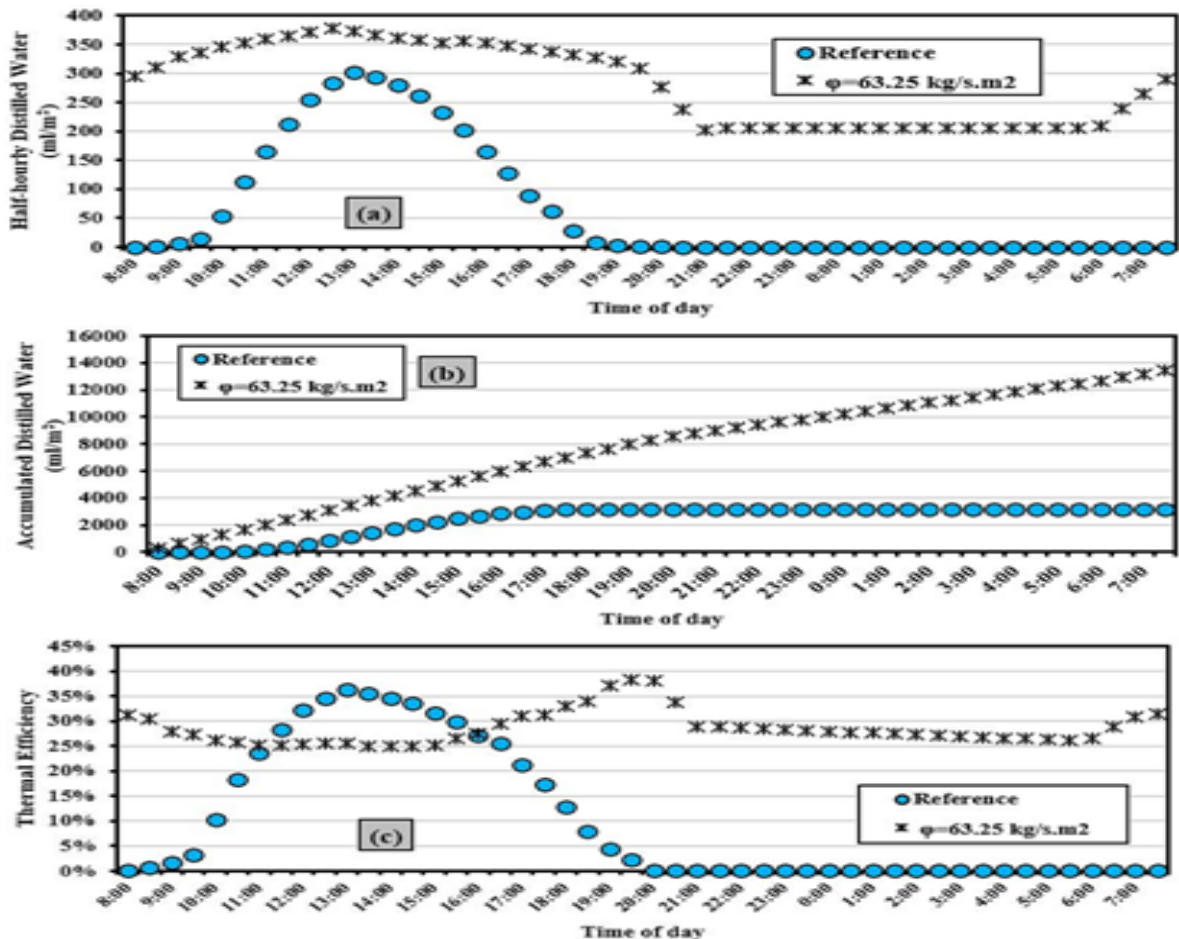


Fig. 8 System performance during 24-hours.

7. Conclusion

In this work, experiments are carried out daily using heating air at several mass fluxes (up to 63.5 kg/s.m²) beneath the solar still unit at constant inlet temperature. The results state that:

- Applying the proposed external heating system augments the accumulated yield while the thermal efficiency is decayed when compared with the unmodified unit.
- Increasing the heating air flow rate boosts both the system productivity and thermal efficiency.
- For the modified unit, the change in the temperatures and freshwater yield are small along the day (24 hours) when compared with the reference one, in which the temperatures reach their peak values at 1 to 1:30 PM.
- The resulted accumulated yield over the whole day (24 hours) is increased from 3.16 l/m² for the reference unit to be 13.48 l/m² with heating air system at mass flux of 63.25 kg/s.m². This increase corresponds to an enhancement ratio of 326.6%.

References

- [1] Mohamed R. Salem, Muataz R. Salem, M.G. Higazy, M.F. Abd Rabbo, "Performance enhancement of a solar still distillation unit: A field investigation", *Solar Energy*, vol. 202, pp. 326-341, 2020.
- [2] World Water Development Report 4. World Water Assessment Programme (WWAP), March 2012.
- [3] M. Abu-Arabia, Y. Zurigat, H. Al-Hinai, S. Al-Hiddabi, "Modeling and performance analysis of a solar desalination unit with double-glass cover cooling", *Desalination*, vol. 143, pp. 173-182, 2002.
- [4] A.M. Radhwan, "Transient performance of a stepped solar still with built-in latent thermal energy storage", *Desalination*, vol. 171, pp. 61-76, 2004.
- [5] E.S. Mettawee, G.M. Assassa, "Experimental study of a compact PCM solar collector", *Energy*, vol. 31, pp. 2958-2968, 2006.
- [6] Z.S. Abdel-Rehim and A. Lashine, "A study of solar desalination still combined with air-conditioning system", *ISRN Renewable Energy*, vol. 2012, Article ID 212496, 7 pages.
- [7] Sandeep, S. Kumar, V.K. Dwivedi, "Enhancing the productivity of modified solar still by cooling the secondary condensing cover", *Desalination*, vol. 367, pp. 69-75, 2015.
- [8] A.A. El-Sebaili, M. El-Naggar, "Year round performance and cost analysis of a finned single basin solar still", *Applied Thermal Engineering*, vol. 110, pp. 787-794, 2016.
- [9] R.S. Hansen, K.K. Murugavel. "Enhancement of integrated solar still using different new absorber configurations: An experimental approach", *Desalination*, vol. 422, pp. 59-67, 2017.
- [10] H.S. Deshmukh, S.B. Thombre, "Solar distillation with single basin solar still using sensible heat storage materials", *Desalination*, vol. 410, pp. 91-98, 2017.
- [11] M. Faegh, M.B. Shafii, "Experimental investigation of a solar still equipped with an external heat storage system using phase change materials and heat pipes", *Desalination*, vol. 409, pp. 128-135, 2017.
- [12] M. Al-harashsheh, M. Abu-Arabi, H. Mousa, Z. Alzghoul, "Solar desalination using solar still enhanced by external solar collector and PCM", *Applied Thermal Engineering*, vol. 128, pp. 1030-1040, 2017.
- [13] S.W. Sharshir, G. Peng, L. Wu, N. Yang, F.A. Essa, A.H. Elsheikh, S. Mohamed, A.E. Kabeel, "Enhancing the solar still performance using nanofluids and glass cover cooling: Experimental study", *Applied Thermal Engineering*, vol. 113, pp. 684-693, 2017.
- [14] D. Rufuss, S. Iniyan, L. Suganthi, D. Pa, "Nanoparticles enhanced phase change material (NPCM) as heat storage in still application for productivity enhancement", *Energy Procedia*, vol. 141, pp. 45-49, 2017.
- [15] O. Mahian, A. Kianifar, S.Z. Heris, D. Wen, A.Z. Sahin, S. Wongwises, "Nanofluids effects on the evaporation rate in a solar still equipped with a heat exchanger", *Nano Energy*, vol. 36, pp. 134-155, 2017.
- [16] M. Shadi, S. Abujazar, S. Fatihaha, E.R. Lotfy, A.E. Kabeel, S. Sharil, "Performance evaluation of inclined copper-stepped solar still in a wet tropical climate", *Desalination*, vol. 425, pp. 94-103, 2018.
- [17] R. Poblete, N.K. Salihoglu, G. Salihoglu, "Optimization of the solar brine evaporation process: Introduction of a solar air heater", *Environmental Progress & Sustainable Energy*, vol. 38, pp. 119-128, 2018.
- [18] A. Kabeel, Y. Taamneh, R. Sathyamurthy, P.N. Kumar, A.M. Manokar, T. Arunkumar, "Experimental study on conventional solar still integrated with inclined solar still under

- different water depth”, Wiley Periodicals, Heat Transfer-Asian Res, vol. 48, pp. 100-114, 2019.
- [19] A.E. Kabeel, M. Abdelgaied, “Enhancement of pyramid-shaped solar stills performance using a high thermal conductivity absorber plate and cooling the glass cover”, Renewable Energy, vol. 146, pp. 769-775, 2020.
- [20] M. Manokar, A.E. Kabeel, R. Sathyamurthy, D. Mageshbabu, B. Madhu, P. Anand, P. Balakrishnan, “Effect of mass flow rate on fresh water improvement from inclined PV panel basin solar still”, Materials Today, vol. 32, pp. 374-378, 2020.
- [21] A.I. Shehata, A.E. Kabeel, M.M. Dawood, A.M. Elharidi, A. Abd_Elsalam, K. Ramzy, A. Mehanna, “Enhancement of the productivity for single solar still with ultrasonic humidifier combined with evacuated solar collector: An experimental study”, Energy Conversion and Management, 208, 112592, 2020.
- [22] W.M. El-Maghlany, A.H. Abdelaziz, A.A. Hanafy, A.E. Kabeel, “Effect of continuous and discrete makeup water on the productivity of conventional solar still”, Journal of Energy Storage, vol. 28, 101223, 2020.
- [23] M.R. Salem, M. Elsayed, A. Abd-Elaziz, K. Elshazly, “Performance enhancement of the photovoltaic cells using Al₂O₃/PCM mixture and/or water cooling-techniques”, Renewable Energy, vol. 138, pp. 876-890, 2019.
- [24] M.R. Salem, “Performance enhancement of a vapor compression refrigeration system using R134a/MWCNT-oil mixture and liquid-suction heat exchanger equipped with twisted tape turbulator”, International Journal of Refrigeration, vol. 120, pp. 357-369, 2020.
- [25] M.R. Salem, “Experimental investigation on the hydrothermal attributes of MWCNT/water nanofluid in the shell-side of shell and semi-circular tubes heat exchanger”, Applied Thermal Engineering, vol. 176, 115438, 2020.
- [26] M.R. Salem, K.M. Elshazly, R.Y. Sakr, R.K. Ali, “Experimental study on convective heat transfer and pressure drop of water-based nanofluid inside shell and coil heat exchanger”, PhD Dissertation, Faculty of Engineering at Shoubra, Benha University, 2014.
- [27] G. Xu, S. Huang, Y. Yang, Y. Wu, K. Zhang, C. Xu, “Techno-economic analysis and optimization of the heat recovery of utility boiler flue gas”, Applied Energy, vol. 112, pp. 907-917, 2013.
- [28] M. Hariprabhu, K. Sundararaju, K.A. Wilson, “Analysis of using exhaust flue gas for power generation in thermal power plant”, International Journal of Pure and Applied Mathematics, vol. 118, pp. 2161-2171, 2018.
- [29] R.W. Miller, “Flow measurement engineering handbook”, 3rd edition, New York: McGraw-Hill, 2000.
- [30] A.E. Kabeel, S.A. El-Agouz, R. Sathyamurthy and T. Arunkumar, “Augmenting the productivity of solar still using jute cloth knitted with sand heat energy storage”, Desalination, vol. 443, pp. 122-129, 2018.

Nomenclatures

A	Area, m ²
C _p	Specific heat, J/kg. °C
H	Height/thickness, m
h _{fg}	Latent heat of vaporization, J/kg
ṁ	Mass flow rate, kg/s
Q	Heat transfer rate, W
T	Temperature, °C or K
t	Time, s
V	Volume, m ³
ṽ	Volume flow rate, m ³ /s

Greek letters

Δ	Differential
η	Efficiency
ρ	Density, kg/m ³

Acronyms and abbreviations

OT	Operating Time
PC	Phase Change Material
M	
SS	Solar Still Unit
U	

Superscripts and subscripts

a	Air
ave	Average
b	Base
c	Collecting
d	Daily
dis	Distilled/daily
g	Glass
h	Hydraulic
I	Instantaneous
i	Inner or inlet or internal
LM	Logarithmic Mean
S	Solar
o	Out or outer
ref	Reference
sw	Saline water
th	Thermal
wv	Water vapor